

## Obtaining thermal and mass diffusivity of the drying process on ceramic plates with the addition of diatomite tailings

Obtenção da difusividade térmica e mássica do processo de secagem sobre tijolos cerâmicos com adição de rejeitos de diatomita

Obtención de difusividad térmica y mássica del proceso de secado sobre placas cerámicas con adición de relaves de diatomeas

Received: 26/06/2022 | Reviewed: 26/07/2022 | Accepted: 28/07/2022 | Published: 05/08/2022

### Raniere Fernandes Costa

ORCID: <https://orcid.org/0000-0002-5831-4251>  
Universidade Federal de Campina Grande, Brazil  
E-mail: [ranierengenharia.costa@gmail.com](mailto:ranierengenharia.costa@gmail.com)

### Alysson Dantas Ferreira

ORCID: <https://orcid.org/0000-0003-0029-8364>  
Universidade Federal de Campina Grande, Brazil  
E-mail: [alysson.dantas@eq.ufcg.edu.br](mailto:alysson.dantas@eq.ufcg.edu.br)

### José Jefferson da Silva Nascimento

ORCID: <https://orcid.org/0000-0002-2620-6491>  
Universidade Federal de Campina Grande, Brazil  
E-mail: [jeffpesquisador@gmail.com](mailto:jeffpesquisador@gmail.com)

### Maria Luiza de Souza Rezende

ORCID: <https://orcid.org/0000-0002-6189-9924>  
Universidade Federal de Campina Grande, Brazil  
E-mail: [mluizarezende@hotmail.com](mailto:mluizarezende@hotmail.com)

### José Jorge da Silva Junior

ORCID: <https://orcid.org/0000-0003-4497-5689>  
Universidade Federal de Campina Grande, Brazil  
E-mail: [josejorge\\_18@hotmail.com](mailto:josejorge_18@hotmail.com)

### Ariadne Soares Meira

ORCID: <https://orcid.org/0000-0001-8740-9009>  
Universidade Federal de Rondonópolis, Brazil  
E-mail: [ariadnesm\\_eng@hotmail.com](mailto:ariadnesm_eng@hotmail.com)

### Antônio Nunes de Oliveira Vieira

ORCID: <https://orcid.org/0000-0001-5697-8110>  
Instituto Federal do Ceará, Brazil  
E-mail: [nunes.vieira@ifce.edu.com](mailto:nunes.vieira@ifce.edu.com)

### Abstract

The drying stage is the most relevant procedure in the industrial production of ceramic bricks, since the final quality of the product is directly related to the success of this operation. Knowledge of the material's thermal and mass diffusivity facilitates mathematical modeling, which brings us a greater domain of the process. With this purpose, the drying of solid ceramic bricks with different percentages of diatomite tailings was experimentally carried out in an oven with forced air circulation. The experiments were performed based on a  $2^k$  experimental design with three factors: the drying temperatures (333 and 383 K), the homogenization time of the mixture (30 and 60 min), and the percentage of tailings (10 and 30%). From the results matrix, we applied the Levenberg-Marquardt algorithm to minimize the difference between the theoretical and the experimental drying and heating curves, thus obtaining the thermal and mass diffusivities. Still in possession of the results matrix, we applied a regression model in order to obtain an equation to estimate the diffusivity values. The drying and heating curves that were built from the estimated diffusivities showed good agreement with the experimental data, and were validated within a 99% confidence interval.

**Keywords:** Drying; Mass diffusivity; Thermal diffusivity; Diffusivity estimated parameters.

### Resumo

A etapa de secagem é o procedimento mais relevante na produção industrial de tijolos cerâmicos, pois a qualidade final do produto está diretamente relacionada ao sucesso desta operação. O conhecimento da difusividade térmica e de massa do material facilita a modelagem matemática, o que nos traz um maior domínio do processo. Para tanto, foi realizada experimentalmente a secagem de tijolos cerâmicos maciços com diferentes porcentagens de rejeitos de

diatomita em estufa com circulação forçada de ar. Os experimentos foram realizados com base em um delineamento experimental de 2k com três fatores: as temperaturas de secagem (333 e 383 K), o tempo de homogeneização da mistura (30 e 60 min) e a porcentagem de rejeitos (10 e 30%). A partir da matriz de resultados, aplicamos o algoritmo de Levenberg-Marquardt para minimizar a diferença entre as curvas de secagem e aquecimento teórica e experimental, obtendo assim as difusividades térmica e de massa. Ainda de posse da matriz de resultados, aplicamos um modelo de regressão para obter uma equação para estimar os valores de difusividade. As curvas de secagem e aquecimento construídas a partir das difusividades estimadas mostraram boa concordância com os dados experimentais e foram validadas dentro de um intervalo de confiança de 99%.

**Palavras-chave:** Secagem; Difusividade de massa; Difusividade térmica; Parâmetros estimados de difusividade.

### Resumen

La etapa de secado es el procedimiento más relevante en la producción industrial de ladrillos cerámicos, ya que la calidad final del producto está directamente relacionada con el éxito de esta operación. El conocimiento de la difusividad térmica y másica del material facilita el modelado matemático, lo que nos aporta un mayor dominio del proceso. Con este propósito, se realizó experimentalmente el secado de ladrillos cerámicos macizos con diferentes porcentajes de relaves de diatomeas en un horno con circulación de aire forzado. Los experimentos se realizaron en base a un diseño experimental 2k con tres factores: las temperaturas de secado (333 y 383 K), el tiempo de homogeneización de la mezcla (30 y 60 min), y el porcentaje de relaves (10 y 30%). A partir de la matriz de resultados, se aplicó el algoritmo de Levenberg-Marquardt para minimizar la diferencia entre las curvas de secado y calentamiento teóricas y experimentales, obteniendo así las difusividades térmica y másica. Todavía en posesión de la matriz de resultados, aplicamos un modelo de regresión para obtener una ecuación para estimar los valores de difusividad. Las curvas de secado y calentamiento que se construyeron a partir de las difusividades estimadas mostraron una buena concordancia con los datos experimentales y se validaron dentro de un intervalo de confianza del 99 %.

**Palabras clave:** Secado; Difusividad de masa; Difusividad térmica; Parámetros estimados de difusividad.

## 1. Introduction

The ceramics industrial sector is quite diversified and can be divided into the following segments: red ceramics, coating materials, refractory materials, sanitary ware, porcelain electrical insulators, tableware, artistic ceramics (decorative and utilitarian), ceramic water filters for domestic use, technical ceramics, and thermal insulators (Abceram, 2017). Red ceramics is a class of reddish colored material used in construction in different forms, such as: hollow and solid bricks, blocks, tiles, flooring, hollow elements, slabs, ceramic pipes, decorative vases, expanded clays, and also household and adornment utensils, among others.

The production of ceramic materials is of great importance in Brazil due to factors such as economic representativeness and job creation, as well as the possibility of co-processing solid waste. This last activity moves about 170 million tons of clay per year (ABDI, 2016), enabling the use of mineral tailings similar to clay, such as diatomite, a biogenic sedimentary rock with high content of natural amorphous silica and small amounts of trace minerals (Macedo *et al.*, 2020; Letelier, 2016). Also called diatomaceous earth, it ends up generating a large amount of tailings in its beneficiation process.

When compared to other porous materials, diatomite offers several advantages: it has excellent mechanical properties such as hardness, corrosion and wear resistance, resistance to chemical attacks, low mass density, durability in aggressive environments and high stability against temperature (Ferrer, 2013). This has caused this material to be investigated in recent years in order to optimize its properties and enhance its uses (Qiu, 2017).

In the production of ceramic materials, it is fundamental to observe the following stages: quarrying, pre-treatment of raw materials, homogenization, drying, and firing.

The thermodynamic process by which the moisture of a solid is reduced by using any appreciable amount of heat energy to evaporate the water and heat the moist solid is called drying. Drying consists on moisture transport from the core to the surface of the material, which can occur in the form of liquid or vapor, depending on the type of solid and the percentage of moisture. In convective drying, the state of the atmospheric air, temperature, relative humidity, and velocity are conditions (predominant parameters) for determining the drying duration (Lima, 2020).

With incorrect drying, the removal of water from the piece is uncontrolled, which can cause structural damage such as cracks, deformations, warping, and consequently a great loss of products. This is why drying operations are important industrial processes, and knowing the mechanism of moisture and heat transfer is of fundamental importance for the ceramic industry. This can be done through a refined and accurate theoretical study, so that the process parameters and their effects on the quality of the final product can be determined (Silva *et al.*, 2011).

Mathematical modeling is the area of knowledge that studies the simulation of real systems in order to predict their behavior, that is, it consists of the attempt to mathematically describe a physical phenomenon (Lima, 2017; Silva, 2018). By means of a suitable mathematical modeling it is possible to properly evaluate the moisture loss and temperature of ceramic products. For this purpose, it is necessary to obtain the solution of the governing equations that compose the model and the creation of computer codes that simulate the heating, water removal, and other effects arising from these processes, aiming to reduce losses and costs.

Once the solution of the governing equations has been found, a comparison with the experimental data must be made in order to verify the consistency of the results obtained and whether the model used was satisfactory, which highlights the importance of experimental studies. This comparison is pertinent to estimate process parameters such as the convective heat and mass transfer coefficients, as well as the thermal and mass diffusivities of the material. The idea is to help control the process, minimize energy consumption, properly design the drying systems, and obtain an optimal quality product. Therefore, knowing the mechanisms of moisture and heat transfer in the product becomes of fundamental importance for the ceramic industry (Nascimento, 2020).

Diffusion is the process of controlling the concentration in space and time of molecules or cells originating from the mixture between reactants, ensuring the development of easily reproducible processes. The process of permeation to gases and water vapor occurs through the empty spaces related to the porosity of the material, that is, in more porous materials the diffusivity is more expressive. The process is considered to take place in different steps: first, sorption and solubilization of the permeant on the surface of the material, followed by diffusion of the permeant through the material due to the action of the concentration gradient, and finally, desorption and evaporation of the permeant on the other face of the material. In the case of ceramic materials, maximum and minimum limits are stipulated for the rate of water absorption and consequent porosity of the product according to the final destination and possible applications. Therefore, it is necessary to control and monitor the main theoretical aspects related to the mechanics and kinetics of diffusion in the products (Ferreira *et al.*, 2018).

In the present study, solid ceramic brick specimens composed of clay with different percentages of diatomite tailings were produced on a laboratory scale in order to evaluate the thermal and mass diffusivities typical of the ceramic material.

## 2. Methodology

For the formulation of the ceramic masses, we used a mixture of *in natura* clay and diatomite tailings. The properties of the material as well as its characterization are found in Costa *et al.* (2021). The manufacturing process of the specimens was divided into the following steps: 1. Preparation of clay and diatomite tailings; 2. Conformation of specimens; 3. Drying; 4. Diffusivity tests.

### Preparation of clay and diatomite tailings

The preparation of the mass proceeded from the drying of raw materials in an oven at 110 °C for 24 hours. Next, the tailings and clay were crushed and mechanically sieved to a passing fraction of 80 mesh for uniformity of the samples. With the sieved grains, they were homogenized in a ball mill for 30 and 60 min, adding 8% humidity to the masses enough to obtain

a good homogenization and reach the plastic point necessary for conformation. We prepared samples with 10 and 30% by mass of diatomite tailings.

### Conformation of the specimens

After the mixing step of the two components, the specimens were conformed by uniaxial pressing in a hydraulic press using a steel matrix and pressure of 20 Mpa, molded in semi-dry mass, with dimensions of 60 x 20 x 5 mm<sup>3</sup>, weight of 11.82 g, and density of 1.97 g/cm<sup>3</sup> as suggested by Medeiros *et al.* (2014).

### Drying of the samples

The samples produced in the pressing step were exposed to drying in order to lose residual moisture remaining from previous steps. The drying of the samples was held in a Marconi air circulation oven with a temperature controller and an operating range between 0 and 200 °C.

We used a galvanized wire tray to accommodate the samples in order to facilitate air circulation above them inside the oven. At pre-established intervals, the samples were taken out of the oven for measurements of their mass, temperature, and dimensions. During the first hour of drying, the samples were taken at 10-minute intervals, after which measurements were taken at 30-minute intervals until the variation in masses stagnated within an accuracy of two decimal places. At the end, in order to obtain the dry mass, the samples were taken to a drying and sterilization (FANEM) without air circulation at 110 °C for 48 hours.

Temperature was measured at the fixed center of each sample, using a thermal gun with a scale ranging from -50 to 1000 °C, TI 890. The dimensions of the specimens were obtained using a Messen digital pachymeter, accurate to 0.01 mm, and the mass was measured on a Quimis BG2000 digital balance, with a deviation of 0.01 g and an error of 0.1 g. Drying was performed in triplicate, each experiment containing five samples of ceramic bricks, and the process conditions followed a 2<sup>k</sup> factorial design. The experiment matrix is presented in Table 1.

### Mass diffusivity modeling

Using the mass variation data of ceramic bricks during drying, the moisture content was calculated from Equation 1:

$$MR = \frac{M_d - M_e}{M_0 - M_e} \quad (1)$$

in which  $M_d$  is the moisture content at time  $t$ ,  $M_0$  is the initial moisture content, and  $M_e$  is the equilibrium moisture, all given in kilograms of water per kilogram of dry matter.

**Table 1** – Experiment matrix of the  $2^k$  factorial design.

	P [%]	T [°C]	H [min]
Experiment 1	10	110	30
Experiment 2	10	110	60
Experiment 3	10	60	30
Experiment 4	10	60	60
Experiment 5	30	110	30
Experiment 6	30	110	60
Experiment 7	30	60	30
Experiment 8	30	60	60

Source: Autors.

With the moisture content over time, drying curves were constructed for each replicate scenario presented in Table 1. We used the Levenberg-Marquardt algorithm to minimize the difference between the experimental data and the theoretical drying curve values from the mass diffusivity.

In order to evaluate the moisture transfer during the drying process of materials, we used Fick's second law. According to Taheri-Garavand *et al.* (2011), in problems involving the drying of ceramic bricks we can adopt the following considerations: (1) moisture is uniformly distributed throughout the mass of the sample; (2) mass transfer is symmetric in relation to the center; (3) moisture contained on the sample surface instantaneously reaches equilibrium with the air in contact; (4) mass transfer resistance at the surface is negligible compared to the internal resistance of the samples; (5) mass transfer occurs only by diffusion; (6) the diffusion coefficient is constant and shrinkage is negligible. This allows us to use Equation 2:

$$MR = \frac{8}{\pi^2} \sum_{n=1}^{\infty} \frac{1}{(2n-1)^2} \exp\left(-\frac{(2n-1)^2 \pi^2 Dt}{4L^2}\right) \quad (2)$$

in which n is the number of terms in the series that will be used, t is the drying time in seconds, D is the effective mass diffusivity of moisture in  $m^2/s$ , and L is the thickness of the brick in meters. According to Lopes *et al.* (2000), only the first term of the series in Equation 2 is used for long drying times, so we should write it as:

$$MR = \frac{8}{\pi^2} \exp\left(-\frac{\pi^2 Dt}{4L^2}\right) \quad (3)$$

### Thermal diffusivity modeling

From the samples' temperature measurement data taken throughout drying, the dimensionless temperature was calculated from Equation 4:

$$\theta = \frac{T_d - T_{\infty}}{T_0 - T_{\infty}} \quad (4)$$

in which  $T_d$  is the temperature of the sample at time t,  $T_0$  is the initial temperature of the sample, and  $T_{\infty}$  is the temperature of the fluid mass exchanging heat with the brick.

Knowing the dimensionless temperatures over time, the heating curves were constructed for each of the replicates of the scenarios listed in Table 1. Similar to what was done in the mass diffusivity modeling, the Levenberg-Marquardt algorithm was used to obtain the thermal diffusivities by minimizing the difference between the experimental data and the theoretical heating curve data.

To evaluate the heating of the bricks during the drying process, we used Equation 5:

$$\theta = 1 - \exp\left[-\frac{hL_c \alpha t}{k L_c^2}\right] \quad (5)$$

in which  $k$  is the thermal conductivity in W/mK,  $\alpha$  is the effective thermal diffusivity of the samples in  $m^2/s$ ,  $L_c$  is the characteristic length and  $h$  is the convection coefficient in  $W/m^2K$ , calculated by:

$$h_c = R_s^{1/2} P_r^{1/3} \frac{k_f}{L_c} \quad (6)$$

According to Incropera (2011), Equation 6 should be used when the conduction heat resistance inside the solid is considered small in comparison to the heat transfer resistance between the solid and its neighborhood. To calculate  $k$ , the percentage of tailings in the sample was taken into account, obtaining a weighted average between the thermal conductivities of clay (0.8364 W/mK) and tailings (0.8956 W/mk).

### Model fitting

The fitting of the model to the experimental data was determined using the statistical parameter of the highest value of the determination coefficient  $R^2$ . The equivalence for this statistical test is given in Equation 7.

$$R^2 = 1 - \frac{\sum_{i=1}^N (MR_{pre,i} - MR_{exp,i})^2}{\sum_{i=1}^N (\overline{MR}_{pre} - MR_{exp,i})^2} \quad (7)$$

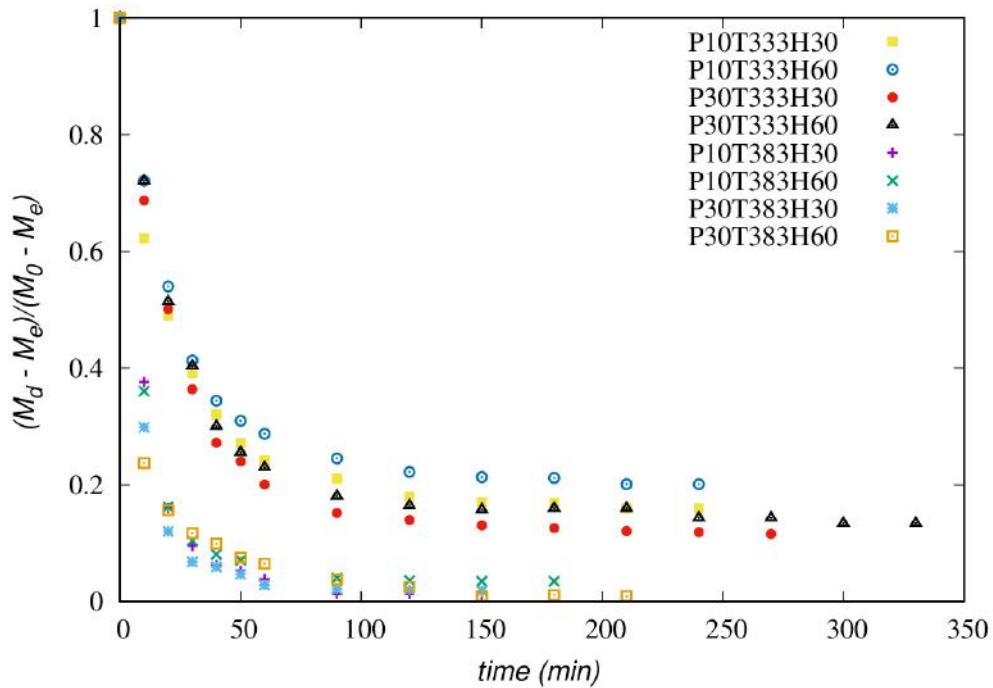
In the equations above,  $MR_{pre,i}$  is the  $i^{th}$  relative humidity obtained from the model,  $MR_{exp,i}$  is the  $i^{th}$  relative humidity obtained from the experimental data,  $N$  is the number of observations, and  $n$  is the number of constants estimated from the experimental data.

## 3. Results and discussion

### Mass diffusion

The drying process was carried out as described in the materials and methods section. From the three replicates performed, we calculated the samples' average mass loss for each of the experiments, and then converted it into moisture content with the help of Equation 1. The result of the average moisture content for each experiment over time is presented in Figure 1.

**Figure 1** – Drying curves of the experiments performed.

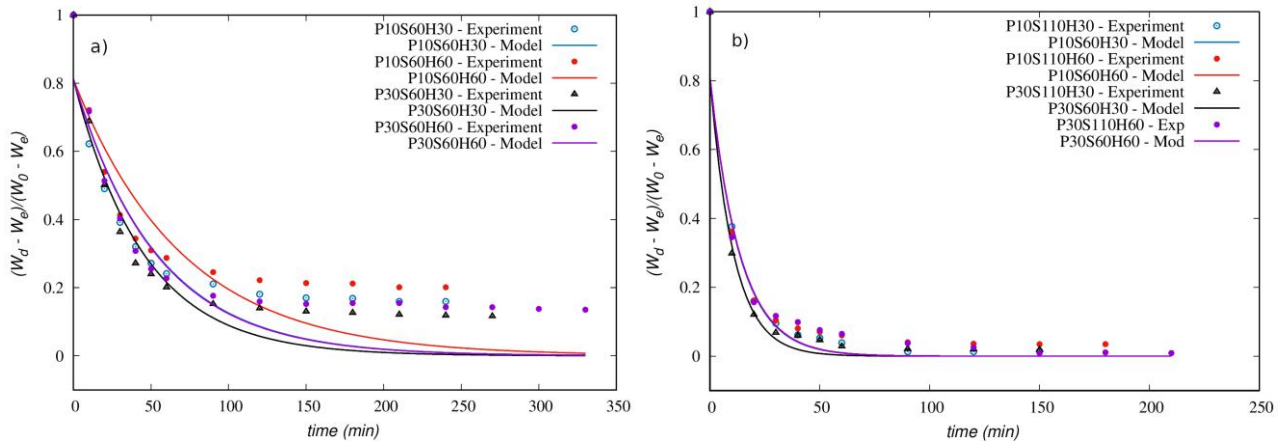


Source: Autors.

Figure 1 shows the drying curves for all eight experiments described in Table 1. In it, we can see how the moisture removal behaves for each of the parameters studied. Also in Figure 1, we can see the influence of temperature on the drying process: the first four curves represent drying at 60 °C, whereas the other curves represent drying at a temperature of 110 °C. This behavior confirms to us that temperature is the main factor that speeds up or slows down the drying time. A second conclusion that we can draw is that the temperature of 60 °C did not provide enough energy to remove all the moisture from the samples, since the moisture contents stabilized around 20%. An analysis of the effects of increasing diatomite tailings and increasing homogenization time can be found in Costa *et al.* 2021.

From the observed behavior of the 60 °C curves, we can say that the model proposed by Equation 3 is not able to predict the behavior of moisture removal, because the model used assumes that the mass transfer resistance of the surface is negligible in relation to the internal resistances of the samples, which would lead to a complete drying of the ceramic bricks (Taheri-Garavand *et al.*, 2011). To confirm this behavior, the drying curves built from the proposed model were plotted and compared to the experimental data for temperatures of 60 °C and 110 °C.

**Figure 2** – Comparison between theoretical drying curves and experimental data a) T = 60 °C, b) T = 110 °C.



Source: Autors.

Analyzing Figure 2-a, we notice that, as expected, the proposed model cannot reproduce the behavior of the 60 °C curves, because the low temperature hinders the evaporation of moisture on the external surface of the bricks, thus increasing the mass transfer resistance of the surface, making it no longer negligible when compared to the internal resistance of the samples, exiting the model's application range. For the 110 °C curves (Figure 2-b), a different behavior is observed. At this temperature, the moisture on the outer surface of the samples is more easily evaporated, making the external mass transfer resistance negligible when compared to the internal resistance, so the model becomes applicable.

Considering the results commented above, the data from the 60 °C curves were removed from the analysis. The degree of agreement, expressed by  $R^2$ , between the experimental data and the model of the drying curves for 110 °C (experiments 1, 2, 5, and 6) is presented in Table 2.

**Table 2** – Results of the coefficient of determination test ( $R^2$ ) for mass diffusivity.

	$R^2$ (%)			
	<i>Exp. 1</i>	<i>Exp. 2</i>	<i>Exp. 5</i>	<i>Exp. 6</i>
<i>R1</i>	93.31	84.51	89.43	71.34
<i>R2</i>	90.91	88.31	88.71	79.22
<i>R3</i>	90.83	85.69	88.46	83.58
<i>Avg.</i>	91.35	86.17	88.87	78.05

Source: Autors.

Observing the average results for all replicates of each experiment considered in Table 2, we verified that the proposed model was able to represent well the experiments, obtaining a minimum average fit of 78.05% for experiment 6.

As shown in Equation 3, it is necessary to use mass diffusivity in the proposed model. For each experiment, this value was estimated using the Levenberg-Marquardt algorithm. The values for each replicate of the experiments considered are shown in Table 6.

**Table 3** – Mass diffusivity values.

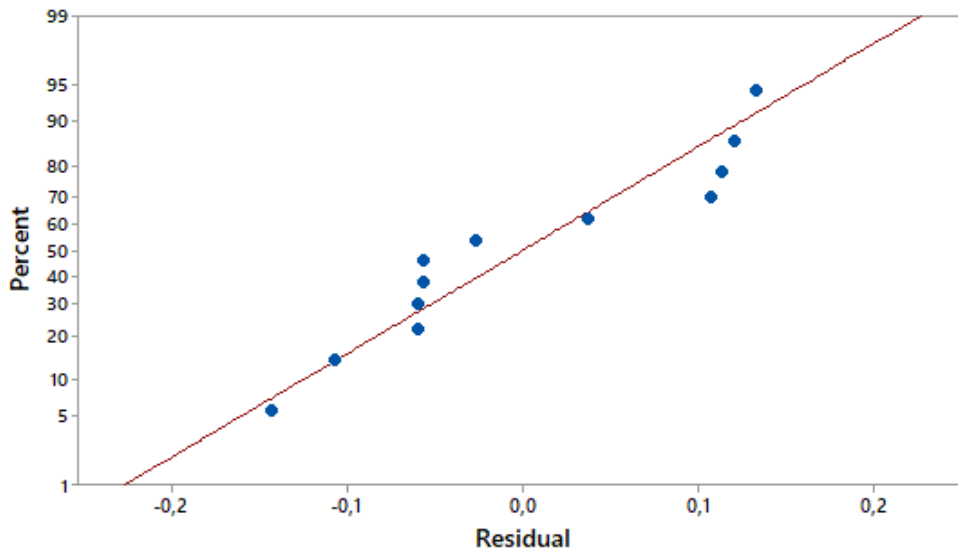
	$D [m^2/s] \times 10^9$		
	R1	R2	R3
Exp. 1	2.44	2.68	2.52
Exp. 2	2.44	2.62	2.44
Exp. 5	3.03	3.21	3.28
Exp. 6	2.63	2.46	2.46

Source: Autors.

In an experimental design, it is necessary to examine the behavior of the residues and check for any violations of the basic assumptions that could invalidate the results. Montgomery (2016) suggests investigating the variance by looking at whether the data are normally and independently distributed. These assumptions must be verified by analyzing the graphs of the residues.

The normal distribution behavior was verified from the normal probability plots shown in Figure 3, while the assumption of independent distribution of variance was verified by plotting the residues versus the fitted values (Figure 4).

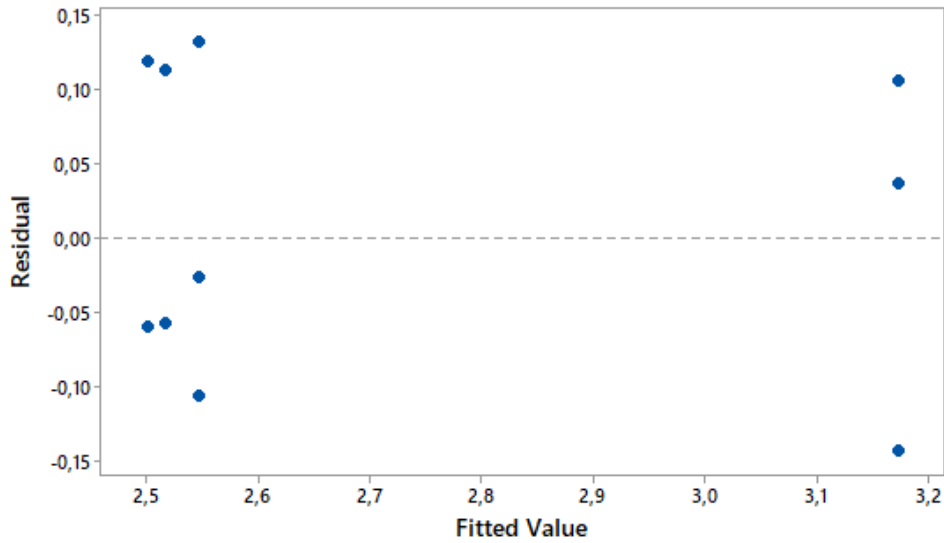
**Figure 3** – Normal probability plot for mass diffusivity.



Source: Autors.

Analyzing the normal probability plots for mass diffusivity, we observe that the experimental data points follow the fitted distribution line, indicating that the normal distribution appears to be a fit for the data. Therefore, we can conclude that the mass diffusivity parameter exhibits normal behavior, thus achieving the Montgomery (2016) recommendation for observations to be normal.

**Figure 4** – Plot of residues versus fitted values for mass diffusivity.



Source: Autors.

Now studying the plot of residues versus fitted values, we observe that the points are randomly distributed on both sides of the line and with no recognizable patterns, indicating that the variance considers the observations to be independently distributed, as recommended by Montgomery (2016).

Based on the estimated values of mass diffusivity (D), and once analysis of variance showed that observations were normal and independently distributed, Equation 8 was developed by fitting a regression model to the data, in order to estimate D as a function of the diatomite tailings mass percentage and the homogenization of the material at a temperature of 110 °C.

$$D = (1.975 + 0.0618P + 0.00861H - 0.001017PH) \times 10^{-9} \quad (8)$$

To evaluate the accuracy of the developed model, we estimated the mass diffusivity value for the conditions presented in Table 4.

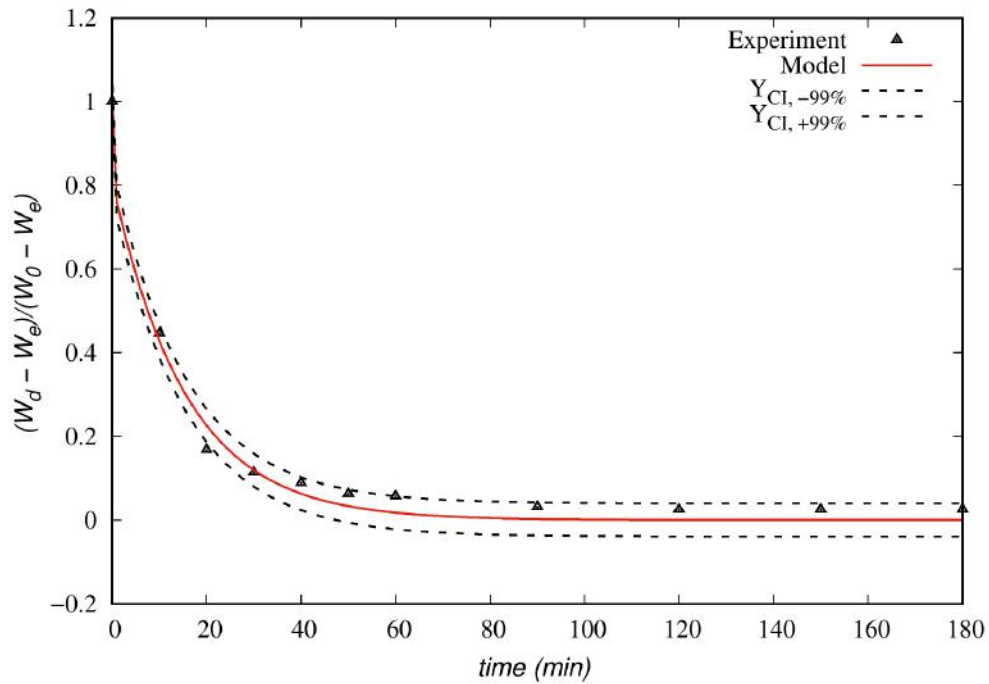
**Table 4** – Parameters for validation of the model developed for mass diffusivity.

	P	T	H	D
<b>Validation</b>	30	110	60	$2.52 \times 10^{-9}$

Source: Autors.

With the estimated value of mass diffusivity, and with the help of Equation 3, we constructed the drying curves for the conditions presented in Table 4. The results of the proposed model were compared to the experimental data, plotting a 99% statistical confidence interval, as presented in Figure 5.

**Figure 5** – Drying curves constructed from the proposed model for mass diffusivity.



Source: Autors.

Analyzing the graph in Figure 5, we can see that the curve generated by the model, with mass diffusivity estimated by Equation 6, presented a good approximation when compared to the experimental data. We also observed that all the experimental points were located within the plotted confidence interval, which ensures greater reliability of the results obtained by the model.

### Thermal diffusion

With the aid of Equation 4, we constructed the samples' heating curves for the experiments presented in Table 1. From Equation 5, the theoretical heating curves were developed. The degree of agreement between the model used and the experimental data was evaluated and placed in Table 5.

**Table 5** – Results of the coefficient of determination test ( $R^2$ ) for thermal diffusivity.

	$R^2$ (%)							
	<i>Exp. 1</i>	<i>Exp. 2</i>	<i>Exp. 3</i>	<i>Exp. 4</i>	<i>Exp. 5</i>	<i>Exp. 6</i>	<i>Exp. 7</i>	<i>Exp. 8</i>
<i>R1</i>	99.29	99.57	97.21	98.61	99.75	99.26	98.68	98.97
<i>R2</i>	98.19	99.02	96.51	97.58	99.72	99.28	98.24	98.51
<i>R3</i>	99.05	99.22	97.57	97.37	99.67	99.07	98.22	97.62
<i>Average</i>	98.84	99.27	97.10	97.85	99.71	99.21	98.38	98.37

Source: Autors.

Looking at the average results for all replicates of each experiment in Table 5, we can see that the proposed model for the samples' heating curve was able to well represent the experiments, obtaining a minimum average fit of 97.10% for experiment 3.

As shown in Equation 5, it is necessary to use mass diffusivity in the proposed model. For each experiment, this value was estimated using the Levenberg-Marquardt algorithm. The values for each replicate of the experiments considered are shown in Table 6.

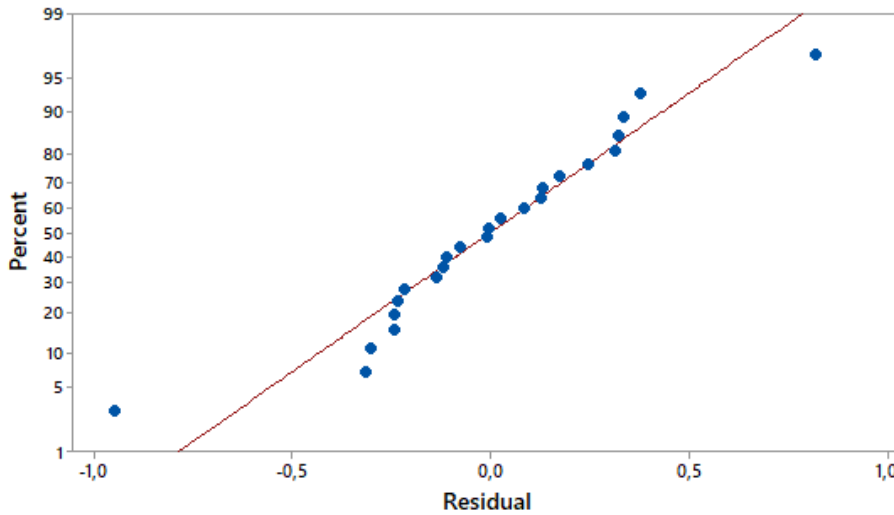
**Table 6** – Thermal diffusivity values.

	$\alpha[m^2/s] \times 10^6$		
	R1	R2	R3
Exp. 1	3.4795	3.3751	3.9927
Exp. 2	3.8128	3.6560	4.2037
Exp. 3	3.5775	3.0243	3.1240
Exp. 4	2.1927	2.6702	2.6206
Exp. 5	4.0407	4.6772	4.3471
Exp. 6	4.5725	5.2597	3.4957
Exp. 7	2.4224	2.4803	2.2855
Exp. 8	2.0178	2.5070	2.2532

Source: Autors.

As reported earlier, we investigated whether there were any violations of the basic assumptions that could invalidate the results, by using the normal probability plots shown in Figure 6, while the assumption of independent distribution of variance was verified by plotting the residues versus the fitted values (Figure 7).

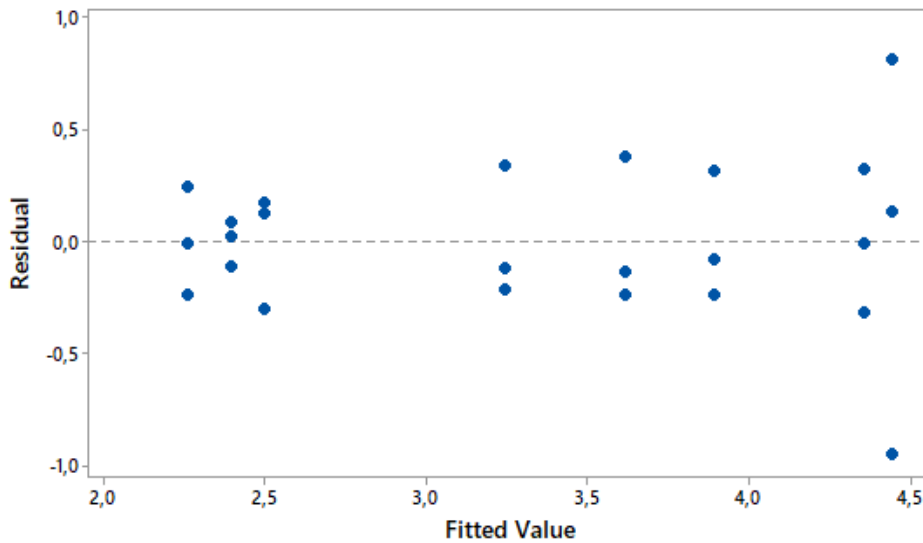
**Figure 6** – Normal probability plot for thermal diffusivity.



Source: Autors.

Observing the normal probability plot for thermal diffusivity, we notice that the experimental data points follow the normal distribution line, but the points at the ends of the x-axis are some distance apart, suggesting a distribution with two outlier points. Therefore, we conclude that the thermal diffusivity parameter shows normal behavior, thus following the Montgomery (2016) recommendation for observations to be normal.

**Figure 7** – Normal probability plot for thermal diffusivity.



Source: Autors.

Now studying the plot of residues versus fitted values, we observe that the points are randomly distributed on both sides of the line and with no recognizable patterns, indicating that the variance considers the observations to be independently distributed, as recommended by Montgomery (2016).

Based on the estimated values of thermal diffusivity ( $\alpha$ ) and having analysis of variance demonstrated that observations were normal and independently distributed, Equation 9 was developed by fitting a regression model to the data, in order to estimate  $\alpha$  as a function of diatomite tailings mass percentage, drying temperature, and material homogenization.

$$\alpha = (6.93 - 0.2158P - 0.0368T - 0.0919H + 0.00238TP + 0.00261PH + 0.000948TH - 0.000027TPH) \times 10^{-6} \quad (9)$$

In order to evaluate the accuracy of the developed model, we estimated the alpha value for the conditions presented in Table 7.

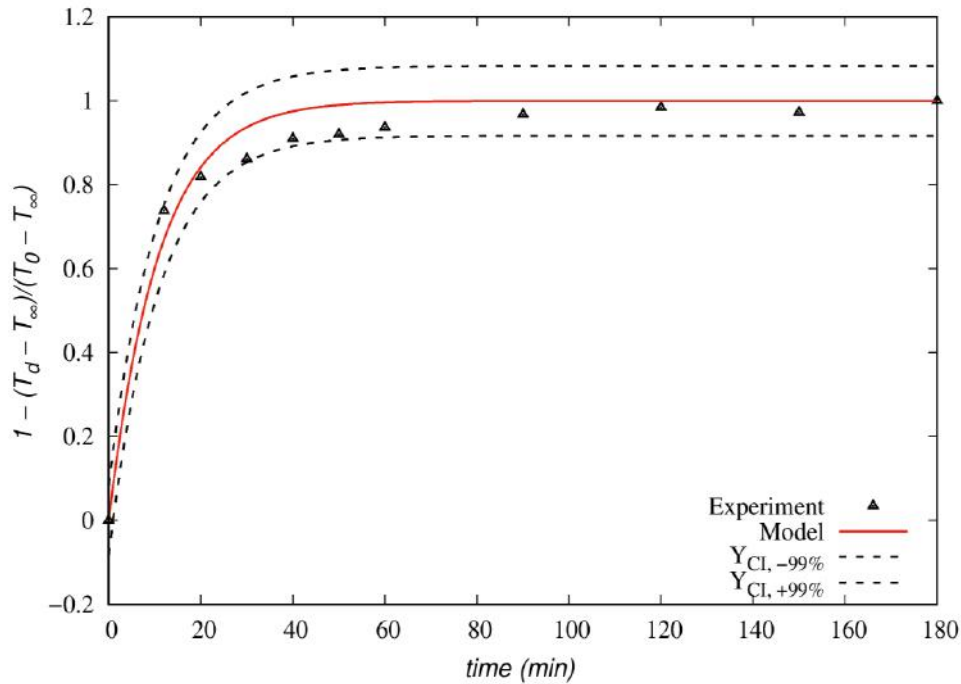
**Table 7** – Parameters for validation of the model developed for thermal diffusivity.

	P	T	H	$\alpha$
<b>Validation</b>	20	80	45	$3.61 \times 10^{-6}$

Source: Autors.

With the estimated value of alpha, and with the aid of Equation 5, we constructed the drying curves for the conditions presented in Table 7. The results of the proposed model were compared to the experimental data, plotting a 99% statistical confidence interval, as presented in Figure 8.

**Figure 8** – Drying curves constructed from the proposed model for thermal diffusivity.



Source: Autors.

Analyzing the graph in Figure 8, we notice that the curve generated by the model, with the thermal diffusivity estimated by Equation 9, showed good approximation when compared to the experimental data. It can also be seen that the experimental points were within the confidence interval, which ensures greater reliability of the results presented by the model.

#### 4. Conclusion

Regarding the results found, we observed that the model proposed for the drying of ceramic bricks was able to represent well the drying curves for the temperature of 110 °C. However, the behavior of the curves at 60 °C did not fit the experimental data, showing that the model cannot be applied for this temperature range.

As for the heating curves, the proposed model showed good representativeness for all temperature ranges of the experimental data, reaching an average degree of fit ( $R^2$ ) of 98.59%.

By means of the experimental design carried out, we noticed that the variance of the experimental data of drying and heating was normal and independent, and thus it was possible to obtain a model to estimate mass ( $D$ ) and thermal diffusivity ( $\alpha$ ) from homogenization time, drying temperature, and percentage of diatomite.

The drying curve obtained from the drying and temperature model, whose diffusivity coefficients were calculated by the equations developed in this research, showed good agreement with the experimental data, hence validating the models.

#### References

- ABCERAM – Associação Brasileira de Cerâmica. *Informações técnicas: definição e classificação*. <https://abceram.org.br/definicao-e-classificacao/>
- ABDI – Agência Brasileira de Desenvolvimento Industrial. (2016). *Estudo técnico setorial da cerâmica vermelha: subsídio para a elaboração do plano de desenvolvimento sustentável da cadeia produtiva de cerâmica vermelha*. Brasília.
- Betsuyaku, R. Y. (2015). *Construção de ecotijolos com adição de areia diatomácea*. Dissertação (Mestrado Profissional em Materiais) – Centro Universitário de Volta Redonda, Volta Redonda- RJ, Brasil.

- Costa, R. F., Ferreira, A. D., Silva Jr, J. J. da., Barbosa, P. M. A., Bandeira, D. J. A., Rezende, M. L. de S., & Nascimento, J. J. da S. (2021). Drying of clay/diatomite hybrid ceramic plates: An experimental study. *Research, Society and Development*, 10(8), e13710817174, 2021. 10.33448/rsd-v10i8.17174.
- Ferrer, M., Peña, G., & Vera, E. (2013). Estrutura, porosidade e resistência mecânica à flexão de cerâmicas porosas feitas com espuma antiderrapante vermelha e poliuretano. *Revista Colombiana de Física*, 45(3), 214-217.
- Incropera, F. P., Dewitt, D. P., Bergman, T. L., & Lavine, A. S. (2014). Fundamentos de transferência de calor e de massa. 7. ed. Rio de Janeiro: LTC.
- Letelier, V., Tarela, E., Muñoz, P., & Moriconi, G. (2016). Assessment of the mechanical properties of a concrete made by reusing both: brewery spent diatomite and recycled aggregates. *Construction and Building Materials*, v. 114, p. 492-498.
- Lima, E.S. de, Lima, W. M. P. B. de, Silva, S. K. B. M. da, Magalhães, H. L. F., Nascimento, L. P. C., Gomez, R. S., Porto, T. R. N., & Lima, A. G. B. de. (2020). Drying of industrial ceramic bricks and process parameter estimation: an advanced concentrated approach. *Research, Society and Development*, 9(12). 10.33448/rsd-v9i12.11391.
- Lima, W. (2017). Transferência de calor e massa em sólidos porosos com geometria complexa via análise concentrada: modelagem e simulação. *Dissertação (Mestrado em Engenharia Mecânica)* – Centro de Ciências e Tecnologia, Universidade Federal de Campina Grande, Campina Grande.
- Lopez, A., Iguaz, A., Esnoz, A., & Virseda, P. (2000). Thin-layer drying behaviour of vegetable waste from wholesale market. *Drying Technology*, 18(4-5), 995-1006. 10.1080/07373930008917749.
- Macedo, A. R. S., Silva, A. S., Da Luz, D. S., Ferreira, R. L. S., Lourenço, C. S., & Gomes, U. U. (2020). Estudo do efeito da diatomita nas propriedades físico-mecânicas do concreto. *Cerâmica*, 66(377), 50-55.
- Medeiros, F. K., Aquino, R. C. A., Rodrigues, A. M. T., Silva, H. C., Dias, I. B. C., & Ferreira, H. S. (2014). Produção de tijolos maciços e placas cerâmicas de revestimento com adição de óleo lubrificante usado. *Cerâmica Industrial*, 19(2), 38-45. 10.4322/cerind.2014.071.
- Monteiro, F. M., Costa, F. A., Machado, T. G., & Assis, R. B. (2017). Caracterização de argila caulínica da região metropolitana de Natal-RN – parte 1. 72º Congresso Anual da ABM. *Anais do Congresso Anual da ABM*.
- Montgomery, D. C., & Runger, G. C. (2016). Estatística aplicada e probabilidade para engenheiros. (6ª. ed.): LTC, 2016.
- Nascimento, L. P. Castanheira; Silva, S. K. B. M., Lima, E. S., Magalhães, H. L. F., Lima, W. M. P. B., Gomez, R. S., Porto, T. R. N., & Lima, A. G. B. (2020). Secagem de tijolos cerâmicos argilosos industriais: uma investigação teórica usando modelos concentrados. *Research, Society and Development*, 9(11). 10.33448/rsd-v9i11.10064.
- Qiu, M., Chen, X., Fan, Y., & Xing, W. (2017). Ceramic membranes. *Comprehensive Membrane Science and Engineering (Second Edition)*, v. 1, p. 270-297. 10.1016/b978-0-12-409547-2.12243-7.
- Silva, J. B., Almeida, G. S., Lima, W. C. P. B., Neves, G. A., & Lima, A. G. B. (2011). Heat and mass diffusion including shrinkage and hygrothermal stress during drying of holed ceramics bricks. *Defect and Diffusion Forum*, v. 312-315, p. 971-976. 10.4028/www.scientific.net/DDF.312-315.971.
- Silva, S. K. B. M. (2018). Secagem de tijolos cerâmicos industriais: estimativa de parâmetros de processo via modelo concentrado. 2018. *Trabalho de Conclusão de Curso (Graduação em Engenharia de Materiais)* – Departamento de Engenharia Mecânica, Universidade Federal de Campina Grande, Campina Grande.
- Taheri-Garavand, A., Rafiee, S., & Keyhani, A. (2011). Study on effective moisture diffusivity, activation energy and mathematical modeling of thin layer drying kinetics of bell pepper. *Australian Journal of Crop Science*, 5(2), 128-131.